Desalination and Water Treatment
www.deswater.com

doi: 10.5004/dwt.2021.27240

226 (2021) 242–250
June

Application of response surface methodology to optimize lead(II) ion adsorption by activated carbon fabricated from de oiled soya

S. Sujatha[a,*], R. Sivarethinamohan[b]

[a]*K. Ramakrishnan College of Technology, Tiruchirapalli, Tamilnadu, India, email: sujalalit@gmail.com*
[b]*Christ (Deemed to be University), Bangalore, Karnataka, India, email: mohan.dimat@gmail.com*

Received 21 August 2020; Accepted 14 March 2021

ABSTRACT

Lead(II) ion a heavy metal is known for its toxicity. An initiative has been taken in this study, to adsorb toxic lead(II) ion using activated carbon made of de oiled soya, by an aqueous solution through batch adsorption methodology. Adsorption process variables such as adsorbent dose, contact time, solution pH, and lead(II) ion concentration were optimized by central composite design (CCD). To find the interaction between process variables, response surface plots were utilized using response surface methodology. Design-Expert software version 7 was resorted to in this experiment. It was observed that the components from the analysis of variance of the CCD revealed that the selective process independent variables had significant control over adsorption capacity. Desirability function was used to appraise the factors and response in adsorption experiments to find an optimum point where the preferred adsorption could be obtained. Adsorption process with the application of activated carbon developed from de-oiled soya meritoriously removed lead(II) ion with an optimum adsorption capacity of 26.279 mg/g for an initial concentration of lead(II) at 60 mg/L.

Keywords: Adsorption; Adsorption capacity; Central composite design; De-oiled soya; Response surface methodology

1. Introduction

Wastewater containing lead, chromium, arsenic, cadmium, and other metals known for their heavy density are termed heavy metals. They are progressively discharged into the surroundings, through anthropogenic activities [1]. Disparate additional pollutants in wastewater, heavy metals are identified as toxic substances. They are non-biodegradable and have extensive half-life [2]. Regardless of the stringent ecological and environmental protocols followed by many countries [3], it is understood that certain heavy metal ions are present in wastewater due to industrial processes. Carrying toxic metal is not a fault but the environment is polluted when metal contaminated wastewater is unintentionally discharged into natural water sources. Hence, terrestrial and aquatic beings including humans face a great menace [4,5]. One of the most dangerous metals is Lead which negatively affects human well-being, mainly children as their developing bodies absorb greater amounts of lead compared to adults [6,7]. Lead is intentionally present in many commercial products such as automobile batteries, utensils, and paints [8,9]. Lead ion in wastewater is harmful in both low and high concentrations. Anaemia, headaches, and diarrhoea, occur in humans due to low level exposure to lead while severe health issues like failure of the kidneys, liver, reproductive, and neurological organs are due to higher concentration of lead in a range of 10 μg/L [10,11]. Lead poisoning may even affect the functioning of the heart and lead to heart failure [12]. Conventional processes to treat wastewater containing heavy metals include membrane filtration, ion exchange, chemical precipitation, floatation, and adsorption. Each method has its own disadvantages with respect to the cost involved in treatment, production of toxic sludge, failure to restore the material used, high

* Corresponding author.

energy demand, and others [13,14]. One of the inexpensive technologies that finds better ways to treat metal contaminated wastewater is adsorption. Adsorption with commercial activated carbon (AC) as an adsorbent go together and are expensive. Hence researchers started searching for inexpensive adsorbents [15]. In general, adsorbents can be any kind of agricultural waste, industrial by products, biomass, biological, and polymeric materials and zeolites [16]. Recently one of the researcher, Cruz-Olivares et al. [17] discovered a brand new adsorbent using gamma irradiated minerals in the year 2016.

Since there is a little gap that exists in discovering new adsorbent, as the water pollution is increasing day by day the authors of this current study indulged themselves in discovering the new adsorbent.

2. Materials and methods

Oil extracted soya bean is called de oiled soya. De oiled soya is a waste product from the soya oil extraction plant located in Tamilnadu, India. Mittal et al. [18] investigated the removal of hazardous Eosin yellow dye using dried de oiled soya by adsorption. The authors have taken this as a base and have already investigated activated carbon of de oiled soya (DOSAC) [19] alternative adsorbent in the removal of hexavalent chromium heavy metals. A experimentation was undertaken here whether DOSAC is suitable to remove lead(II) ion.

Since it is a waste, author DOSAC's adsorptive action of activated carbon is permeable and can remove many dissolved impurities and heavy metals in water. Initially de oiled soya bean was crushed into small pieces and cleansed with distilled water. It was further dehydrated in an oven till it was completely dry. It was then treated with a hydrogen peroxide solution (30% w/v) for 24 h at room temperature [18]. A muffle furnace was used to convert the dehydrated de oiled soya bean into DOSAC. Figs. 1 and 2 portray the de oiled soya bean and its activated carbon (DOSAC).

Fabricated DOSAC (de oiled soya activated carbon) underwent characterization studies including scanning electron microscopy (SEM), Fourier transform infrared spectroscopy (FTIR), and X-ray diffraction (XRD) analyses to understand its adsorption properties The current study contributes to the preparation of a derivative (an activated carbon) from de-oiled soya (DOSAC) to treat lead(II) ion infested water by the batch adsorption mode. Optimum condition for four process variables like initial concentration of lead(II), its pH, lead(II) ionic wastewater, interaction time of the investigation and DOSAC (adsorbent) dosage were tested and determined with the help of central composite design (CCD) [20–22] rotatable under response surface methodology (RSM) by using Design Expert software version 7.

3. Results and discussions

3.1. Characterization of DOSAC

3.1.1. SEM and FTIR analyses

Fig. 3a is the SEM image of DOSAC before adsorption revealed the presence of a porous, irregular surface that enabled desorption of lead(II) ions onto the adsorbent. Space which was advantageous for adsorption to occur was also revealed. Rough surface and numerous pores ensured diffusion paths for ions to enter carbons [23]. Further physical adsorption seriously affected the exclusion of lead(II) ion from the aqueous solution. The microscopic image in Fig. 3b reveals that the pores were occupied by lead(II) ions thereby reducing the number of pores on the carbon's surface.

It is seen from Fig. 4a that the FTIR spectrum of DOSAC comprised a peak at 3,339 cm^{-1} [24] which could be denoted presence of C–H aliphatic [24] acids in AC. It was further found that 1,651 cm^{-1} related to C=C [25,26] stretch alkenes. The peak 1,603 cm^{-1} referred to C=O (carbonyl group) stretch of aromatic groups such as primary and secondary amides [27,28]. The peak 1,113–1,161 cm^{-1} [28] unveiled the presence of the C–O stretching alcohols, and carboxylic acid in the adsorbent. Also, peaks between 700 and 753 cm^{-1} could be due to C–H aromatic rings [26,28].

It was well-understood from Fig. 4b that there was shift in the peaks after adsorption took place in DOSAC.

The pattern of crystals in DOSAC endorsed the peak revealed in Fig. 5 through XRD analysis. This was through the distribution of atoms within the DOSAC lattice. Reduced

Fig. 1. De oiled soya bean [19].

Fig. 2. DOSAC [19].

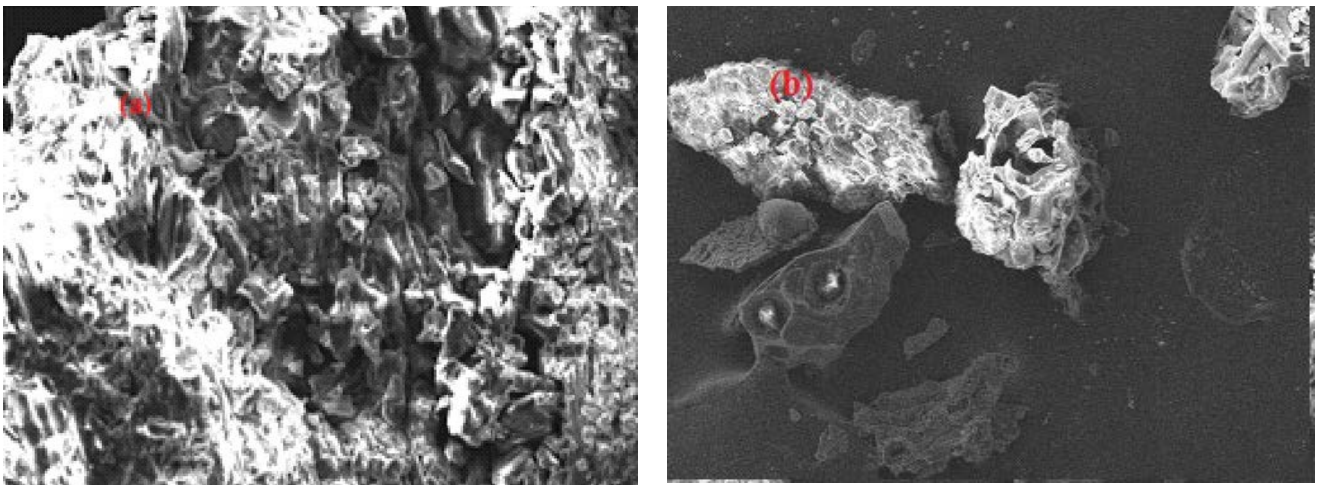

Fig. 3. SEM photograph of (a) DOSAC and (b) lead(II) loaded DOSAC.

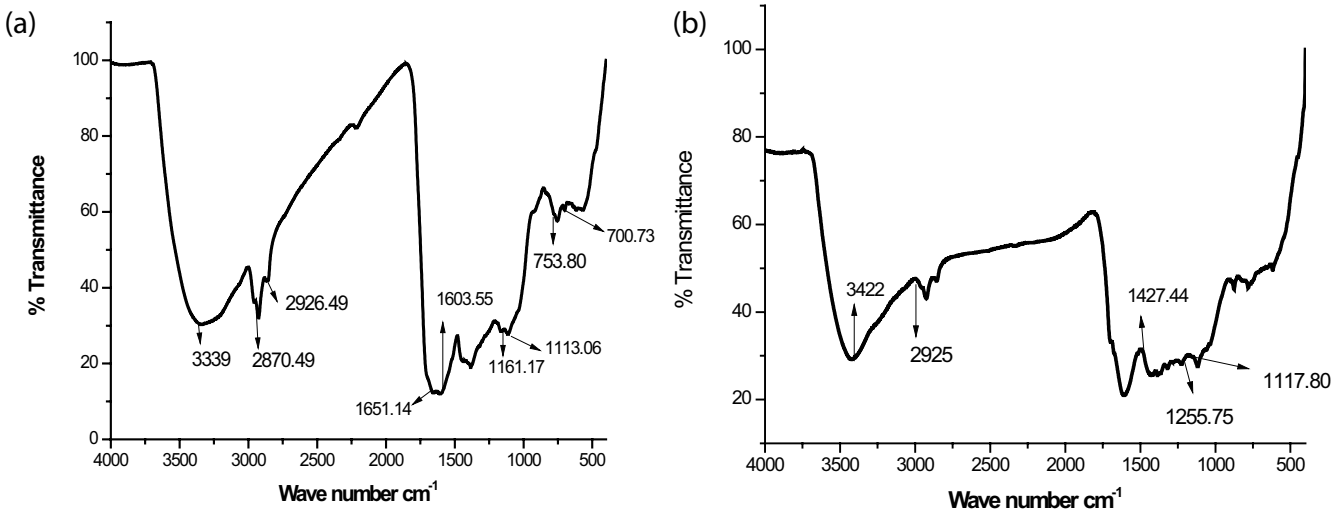

Fig. 4. FTIR continuum of DOSAC: (a) before and (b) after adsorption.

number of peaks in Fig. 5 revealed that the developed carbons were amorphous in nature. Peaks observed in XRD patterns 2θ = 25° and 48° in DOSAC were due to the presence of faujasite and sodium silicates [29], respectively.

3.1.2. Estimation of pH of zero charge-point of zero charge

The point of zero charge (pzc) is the pH at which the surface of your adsorbent is globally neutral, that is, contains as much positively charged as negatively charged surface functions. The pH of the 0.01 M NaCl was adjusted to a value between 2 and 10 using 0.5 M HCl or 0.5 M NaOH. An adsorbent (0.5 g) was added to 20 mL of the pH adjusted solution in a capped vial and equilibrated for 24 h. The final pH was measured and plotted against the initial pH. The pH at which the curve crosses the $pH_{initial}$ = pH_{final} line was taken as the pzc. Fig. 6 depicts the pzc plot. It is found that pzc is occurred at 4.02 pH.

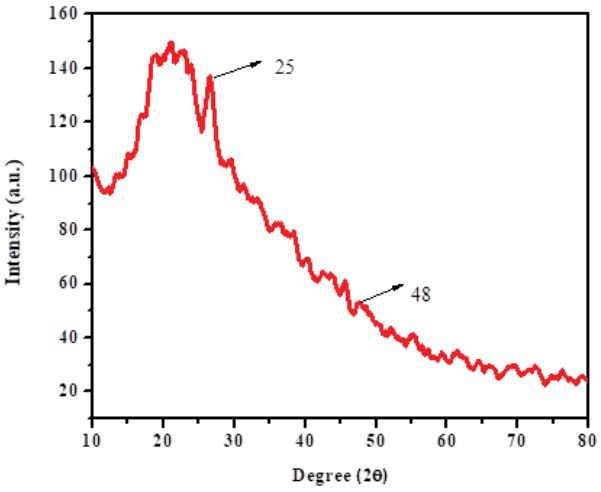

Fig. 5. Spectrum-XRD of DOSAC.

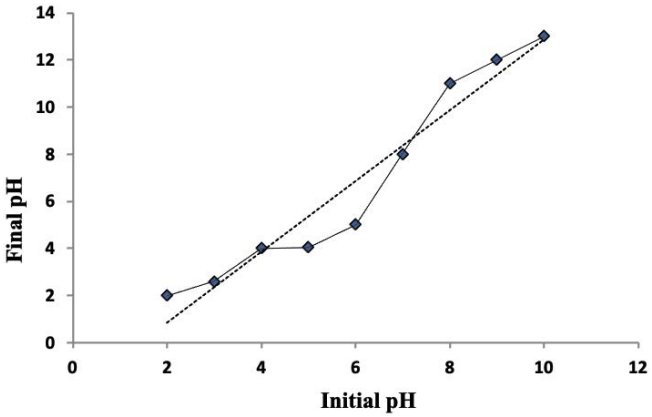

Fig. 6. Point of zero charge.

3.1.3. Isotherm and kinetic studies

The Langmuir adsorption and the Freundlich adsorption isotherm model fit was analysed with experimental data. Similarly kinetic models were analysed. It was very clear from Table 1 adsorption isotherm models Langmuir and Freundlich perfectly fit the adsorption of lead(II) with DOSAC. Whereas the second-pseudo-kinetic model fit perfectly with the adsorption than that of the first order model.

In general it could be reflected from the kinetic studies that the transfer of adsorbate from bulk solution to adsorbent surface was through diffusion and there was migration of adsorbate into pores of the adsorbent.

3.2. CCD for the batch adsorption experiment

CCD provides [20,21] information on a multilevel factorial which need fewer experiments [22] than a full factorial which is sufficient to describe the majority of responses. Ideal values of the process variables for adsorption were calculated using the fitted models and validated by experiments. Different process variables and their ranges used in the model's computation were 40 and 60 mg/L for lead(II) ion concentration. The lower and upper limits of pH were 4 and 6. Similarly the adsorbent dose was 0.2 and 0.4 g and the contact time 60 and 80 min. This experimental work employed nine combination of test variables namely A, B, C, D, AB, AC, AD, BC, BD, CD, A^2, B^2, C^2, and D^2. A was the Initial concentration, B was the pH, C was the adsorbent dose, and D was the contact time.

Table 1
Adsorption isotherm constants and pseudo kinetic adsorption constants of lead(II) adsorption

Langmuir constants		Pseudo-first-order kinetics	
Q_0 (mg/g)	18.182	k_1 (min^{-1})	0.0183
b (L/mg)	0.237	R^2	0.732
R_L	0.095	q_e (mg/g)	3.572
R^2	0.991		
Freundlich constants		Pseudo-second-order kinetics	
K_f (mg/g)	4.256	k_2 (min^{-1})	0.0108
n	2.544	R^2	0.986
R^2	0.802	q_e (mg/g)	13.698

3.2.1. Mathematical model development

Design Expert Software represented a four factor quadratic polynomial model for the adsorption of lead(II) ion by DOSAC as portrayed in [30] Table 2.

It is understood from Table 3 that the quadratic model is significant for the current study. This is supported by the predicted R-squared value nearing 1 (0.987592) [31] in Table 2.

From Table 4, the model's F-value of 679.54 was found to be significant. There was only a 0.01% chances that F-value was large which could be due to noise. Values of "Prob > F" less than 0.0500 indicated that the model's terms were significant. Here A, B, C, D, AB, AC, AD, BD, CD, A^2, B^2, and C^2 are significant model terms. Left behind source term values, greater than 0.1000 signified their insignificance and hence were removed. The "lack of fit F-value" shows that the lack of fit was not significant revealing that model reduction might improve the model.

$$\text{Adsorption capacity } Y = 12.008 + 2.807 \times A - 0.551 \times B - 5.115 \times C + 0.613 \times D - 0.232 \times A \times B - 0.724 \times A \times C + 0.628 \times A \times D - 0.478 \times B \times D - 0.412 \times C \times D + 0.268 \times A^2 - 0.209 \times B^2 + 2.694 \times C^2 \quad (1)$$

Eq. (1) with coded variables was able to verbalize by referring to the reaction for a given unit in each factor. The upraised levels of the process variables were reported as +1 and the variable truncated units as –1. Equally indicated by the conditions, initial concentration, and contact time positively affected lead(II) retention, whereas pH and

Table 2
Sequential model sum of squares for model evaluation

Source	Sum of squares	df	Mean square	F-value	p-value Prob. > F	Inference
Mean vs. total	5,422.8	1	5,422.8			
Linear vs. mean	844.6	4	211.1	32.4	<0.0001	
2FI vs. linear	27.5	6	4.6	0.6	0.7044	
Quadratic vs. 2FI	107.8	4	26.9	203.8	<0.0001	Model suggested
Cubic vs. quadratic	1.1	6	0.2	3.1	0.1193	Model aliased
Residual	0.3	5	0.1			

Table 3
Model summary statistics

Source	Standard deviation	*R*-squared	Adjusted *R*-squared	Predicted *R*-squared	Press	Results
Linear	2.55	0.860624	0.834076	0.777635	218.2245	
2FI	2.70	0.888682	0.814469	0.654228	339.3327	
Quadratic	0.36	0.998518	0.996632	0.987592	12.17682	Suggested
Cubic	0.25	0.999684	0.998419		+	Aliased

Table 4
ANOVA for response surface reduced quadratic model for lead(II) adsorption by DOSAC

Source	SS	df	MS	*F*-value	*p*-value Prob. > *F*	Inference
Model	979.82	12	81.65	679.54	<0.0001	Significant
A	119.30	1	119.3	992.86	<0.0001	
B	6.64	1	6.64	55.26	<0.0001	
C	372.44	1	372.4	3,099.58	<0.0001	
D	6.49	1	6.49	53.99	<0.0001	
AB	0.75	1	0.75	6.24	0.0267	
AC	7.31	1	7.31	60.84	<0.0001	
AD	5.50	1	5.50	45.77	<0.0001	
BD	3.18	1	3.18	26.45	0.0002	
CD	2.36	1	2.36	19.65	0.0007	
A^2	1.03	1	1.03	8.54	0.0119	
B^2	1.13	1	1.13	9.42	0.0090	
C^2	98.82	1	98.82	822.38	<0.0001	
Residual	1.56	13	0.12			
Lack of fit	1.25	8	0.16	2.52	0.1617	Not significant

adsorbent portion affected it the other way. Adsorption capacity increased with an escalating initial concentration. Also when pH increased with the adsorbent dose, adsorption rate diminished. The three dimensional reaction surface plots are given in Fig. 7. As the concentration of lead(II) ion increased from 40 to 60 mg/L pH diminished from 6 to 4 while adsorption limit increased. High starting fixation of the initial concentration and the stumpy pH estimate indicated an addition in the adsorption limit. When pH expanded, adsorption did not. In like manner, high adsorbent dose did not support adsorption of DOSAC as depicted in Fig. 6. Delineated low pH and increased contact time resulted in DOSAC's impressive adsorption limit.

In this plot Fig. 8, the normal % probability are plotted along the horizontal *x*-axis; the vertical *y*-axis shows the internally studentized residuals for the respective values. Internally studentized residuals take into account the inequality of variances across the factor space, and any value outside 3 is a possible outlier. The limit of the internally studentized residuals found in diagnostic case statistics for adsorption with DOSAC was ±3 sigma [20]. This is a signal of better agreement of the model with the experimental data.

The analytic plot predicted vs. actual adsorption capacity was intended to evaluate the appropriateness of the created numerical model. There was utilized to assess the fit of the relapse model. The connection between the real and anticipated adsorption limits is shown in Fig. 9. Further, it assigns a relationship between the information found through tests and the estimates anticipated by the regression model for the adsorption process in evacuating lead(II).

3.2.2. Optimization of the process variable

Design Expert provides five probable objectives to pick the ideal for every factor and reaction. In the current experimentation, desired response – adsorption capacity was set as maximum and "in the range" desirability was agreed upon for four independent variables like initial concentration, pH, contact time, and DOSAC dose. The desirability plot in Fig. 8 enabled us to visualize the desirability for the process variable and output.

It is seen from Fig. 10 that the desirability value was 1 for the individual and a combination of all process variables at a maximum of 0.735 was developed from DOSAC for lead(II) removal. Desirability analysis from the RAMP plot (Fig. 11) provided the inference about the optimum response regarding the adsorption capacity of DOSAC as 26.279 mg/g when process variables were 60 mg/L (initial concentration), 4.03 (pH), and 0.2 g (DOSAC dose) for a contact time of 80 min at a desirability value of 0.741.

3.3. D–R isotherm

The D–R adsorption isotherm model was applied on the experimental data. It is common to apply Eq. (2) [32]:

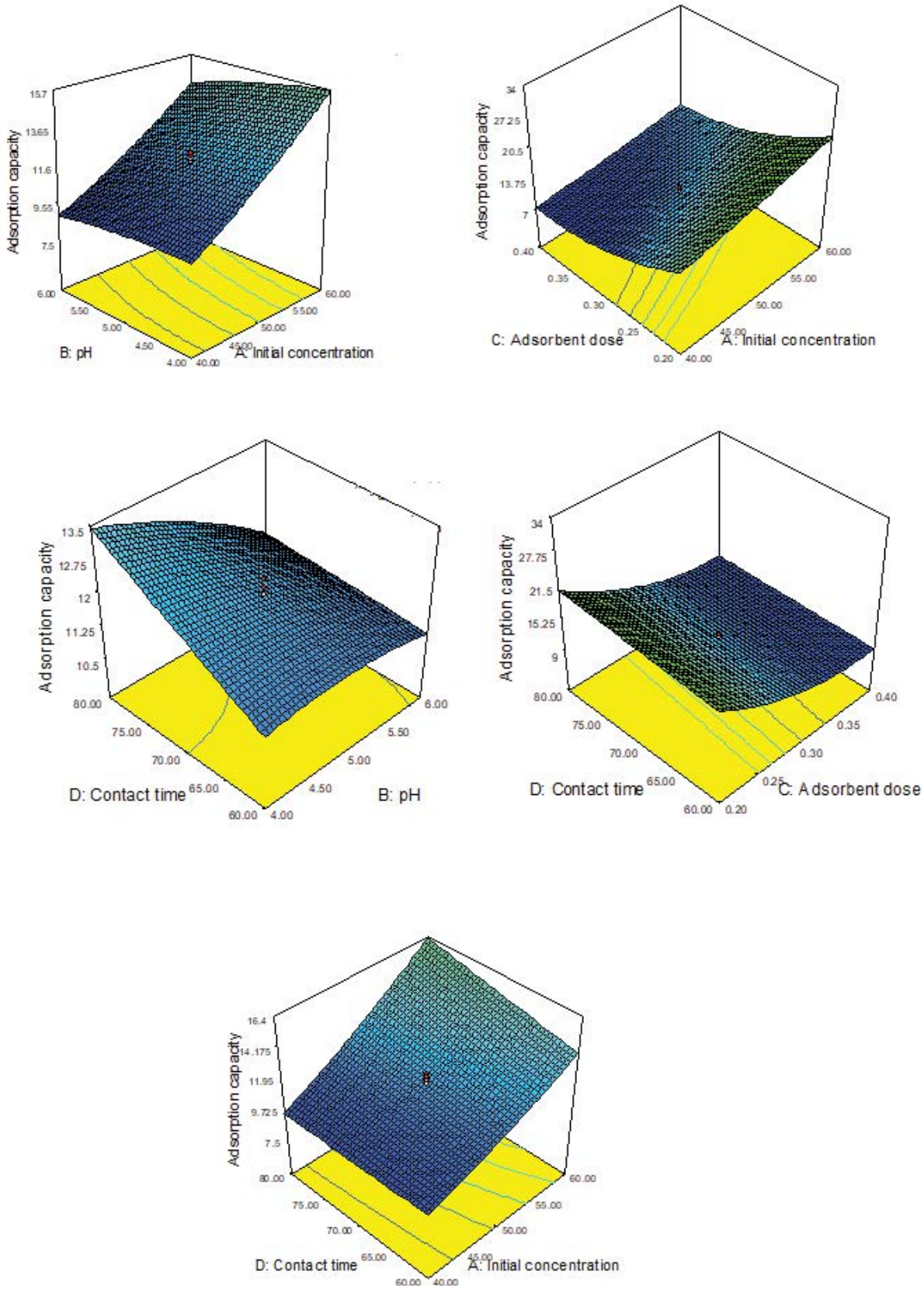

Fig. 7. Upshot of interface connecting the variables under consideration.

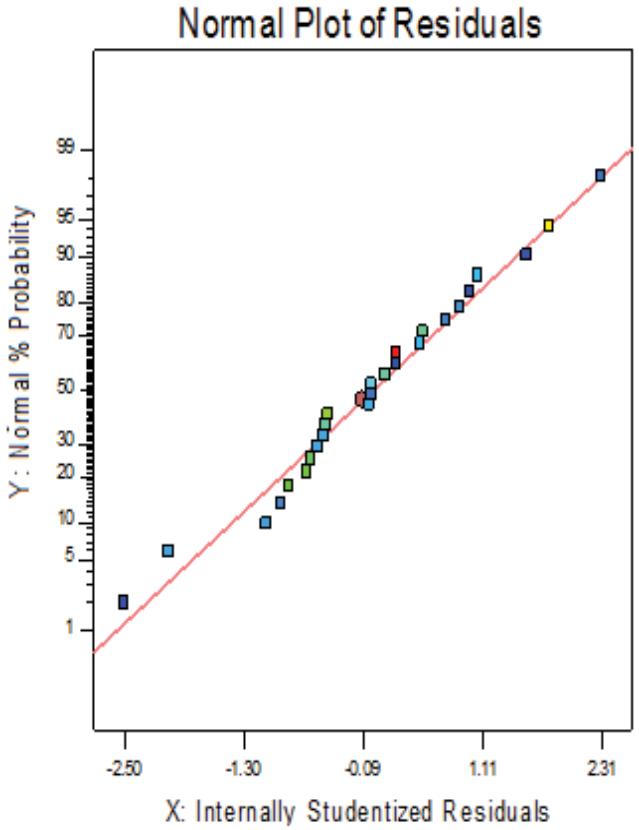

Fig. 8. Normal probability plot of studentized residuals for adsorption of lead(II) by DOSAC.

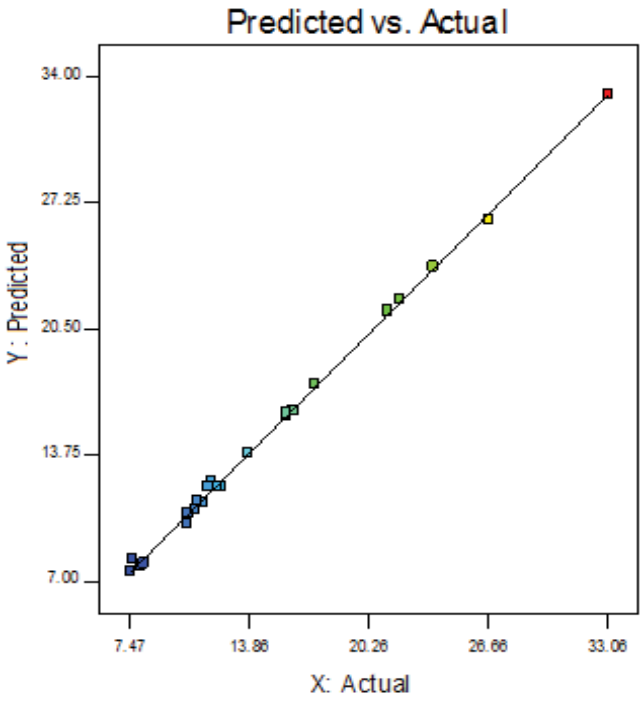

Fig. 9. Interface connecting the actual and predicted figures of adsorption capacity.

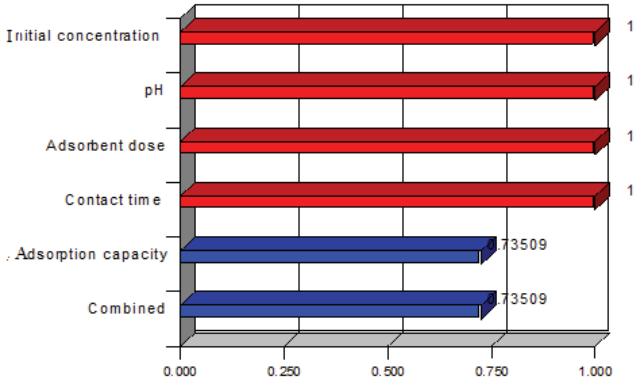

Fig. 10. Desirability plot for adsorption of lead(II) by DOSAC.

$$\ln\left(q_e\right) = \ln\left(q_s\right) - K_{\text{ad}}\varepsilon^2 \tag{2}$$

where q_s is the theoretical isotherm saturation capacity in mg/g and K_{ad} is the D–R isotherm constant (mol^2/kJ^2). ε is the D–R isotherm constant and is calculated using the following relationship [30]:

$$\varepsilon = RT\ln\left[1+\frac{1}{C_e}\right] \tag{3}$$

where R, T, and C_e represent the gas constant (8.314 J/mol K), absolute temperature (K) and lead equilibrium concentration (mg/L), respectively. A plot (Fig. 12) is drawn between $\ln q_e$ vs. ε^2 square of the potential energy. From the linear plot, q_s were determined to be 18.1 mg/g and E the mean adsorption energy in kJ and is calculated using Eq. (4):

$$E = \frac{1}{\sqrt{-2K_{\text{ad}}}} \tag{4}$$

It was found that E is 0.791 kJ indicates the physisorption process has taken place in the adsorption.

4. Conclusion

In the current study, adsorption performance of DOSAC fabricated from De oiled soya in the removal of lead(II) was studied with focus on the impact of process variables by the application of RSM with CCD. The result of the study revealed that RSM was an appropriate method to optimize the operating conditions in removing lead(II). Response surface plots developed to determine lead(II) adsorption capacity were appropriate. Analysis of variance (ANOVA) showed a high coefficient of determination value (R^2 = 0.987592), which ensured that four factor quadratic polynomial models were best suited for the experiment under consideration. D–R isotherm indicates the existence of physisorption in this study. Optimum adsorption capacity was 26.279 mg/g with optimum process variables including 60 mg/L initial concentration,

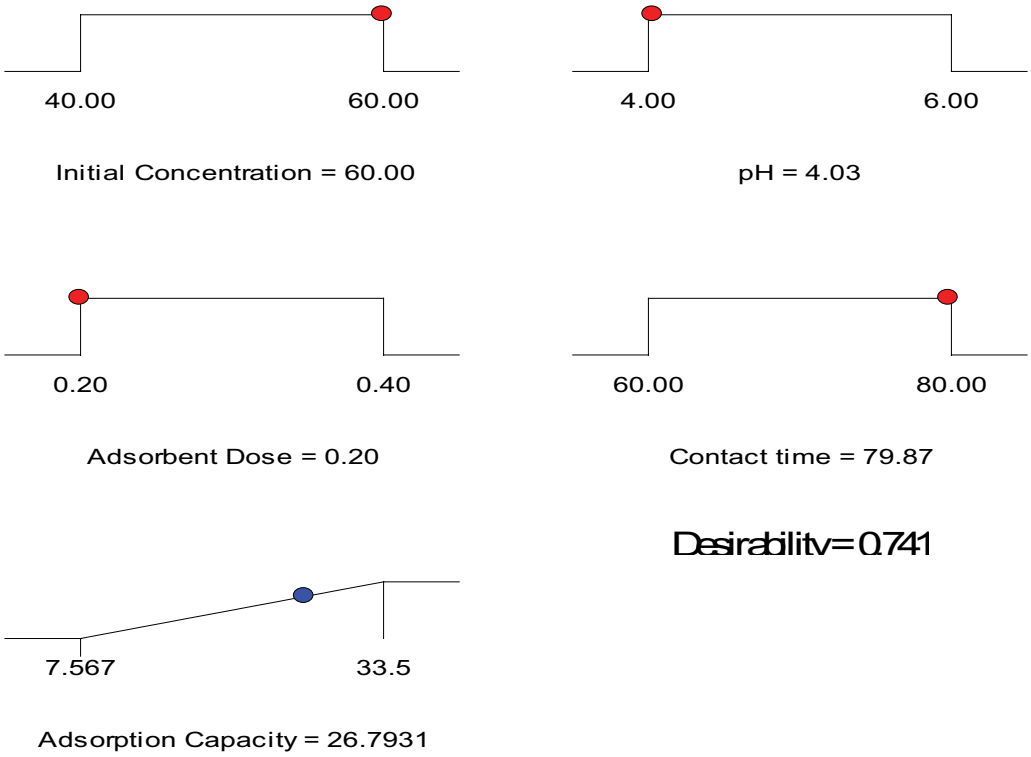

Fig. 11. RAMP plot for adsorption of lead(II) – DOSAC.

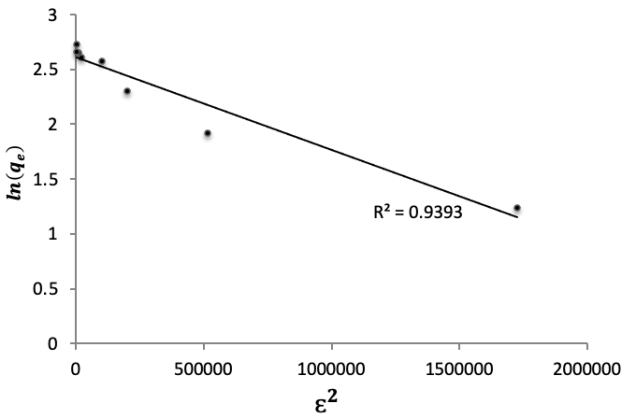

Fig. 12. D–R isotherm.

4.03 (pH), 0.2 g (DOSAC dose), and contact time of 80 min for a desirability value of 0.741. From the environment point of view, this finding will have a substantial impact in removing lead(II) in aqueous solutions using DOSAC activated carbon fabricated from de oiled soya.

References

[1] F. Fu, Q. Wang, Removal of heavy metal ions from wastewaters: a review, J. Environ. Manage., 92 (2011) 407–418.
[2] I.U. Salihi, S.R.M. Kutty, M.H. Isa, N.N. Aminu, Zinc removal from aqueous solution using novel adsorbent MISCBA, J. Water Sanit. Hyg. Dev., 6 (2016) 377–388.
[3] M. Greenstone, R. Hanna, Environmental regulations, air and water pollution, and infant mortality in India, Am. Econ. Rev., 104 (2014) 3038–3072.
[4] S. Demim, N. Drouiche, A. Aouabed, S. Semsari, CCD study on the ecophysiological effects of heavy metals on *Lemna gibba*, Ecol. Eng., 57 (2013) 302–313.
[5] M. Jaishankar, T. Tseten, N. Anbalagan, B.B. Mathew, K.N. Beeregowda, Toxicity, mechanism and health effects of some heavy metals, Interdiscip. Toxicol., 7 (2014) 60–72.
[6] R.L. Canfield, C.R. Henderson, D.A. Cory-Slechta, C. Cox, T.A. Jusko, B.P. Lanphear, Intellectual impairment in children with blood lead concentrations below 10 microg per decilitre, N. Engl. J. Med., 348 (2003) 1517–1526.
[7] A. Chen, K.N. Dietrich, J.H. Ware, J. Radcliffe, W.J. Rogan, IQ and blood lead from 2 to 7 years of age: are the effects in older children the residual of high blood lead concentrations in 2-year-olds, Environ. Health Perspect., 113 (2005) 597–601.
[8] J.D. Weidenhamer, P.A. Kobunski, G. Kuepouo, R.W. Corbin, P. Gottesfeld, Lead exposure from aluminum cookware in Cameroon, Sci. Total Environ., 496 (2014) 339–347.
[9] P. Gottesfeld, Time to ban lead in industrial paints and coatings, Front. Public Health, 3 (2015) 1–4.
[10] L. Charlet, Y. Chapron, P. Faller, R. Kirsch, A.T. Stone, P.C. Baveye, Neurodegenerative diseases and exposure to the environmental metals Mn, Pb, and Hg, Coord. Chem. Rev., 256 (2012) 2147–2163.
[11] N. Arancibia-Miranda, S.E. Baltazar, A. Garcia, D. Munoz-Lira, P. Sepulvedaa, M.A. Rubioa, D. Altbir, Nanoscale zero valent supported by Zeolite and Montmorillonite: template effect of the removal of lead ion from an aqueous solution, J. Hazard. Mater., 301 (2016) 371–380.
[12] G.F.D. Mattos, C. Costa, F. Savio, M. Alonso, G.L. Nicolson, Lead poisoning: acute exposure of the heart to lead ions promotes changes in cardiac function and Cav1.2 ion channels, Biophys. Rev., 9 (2017) 807–825.

[13] H. Eccles, Treatment of metal-contaminated wastes: why select a biological process?, Trends Biotechnol., 17 (199) 462–465.
[14] P. Chowdhary, A. Yadav, G. Kaithwas, R.N. Bharagava, Distillery Wastewater: A Major Source of Environmental Pollution and Its Biological Treatment for Environmental Safety, R. Singh, S. Kumar, Eds., Green Technologies and Environmental Sustainability, Cham, Springer, 2017a, 409–435.
[15] Y.S. Mohammad, S.B. Igboro, A. Giwa, C.A. Okuofu, Modeling and optimization for production of rice husk activated carbon and adsorption of phenol, J. Eng., 201 (2014) 1–10.
[16] T.A. Kurniawan, G.Y.S. Chan, W.-h. Lo, S. Babel, Comparisons of low-cost adsorbents for treating wastewaters laden with heavy metals, Sci. Total Environ., 366 (2006) 409–426.
[17] J. Cruz-Olivares, G. Martínez-Barrera, C. Perez-Alonso, C.E. Barrera-Díaz, M.D.C. Chaparro-Mercado, F. Ureña-Núñez, Adsorption of lead ions from aqueous solutions using gamma irradiated minerals, J. Chem., 2016 (2016) 1–7, doi: 10.1155/2016/8782469.
[18] A. Mittal, D. Jhare, J. Mittal, Adsorption of hazardous dye Eosin Yellow from aqueous solution onto waste material de-oiled soya: isotherm, kinetics and bulk removal, J. Mol. Liq., 179 (2013) 133–140.
[19] S. Sujatha, G. Venkatesan, R. Sivarethinamohan, Principal determinants of toxicity reduction by de-oiled soya using multivariate statistics: principal component analysis and multiple linear regression analysis, Appl. Ecol. Environ. Res., 15 (2017) 1717–1737.
[20] B. Sadhukhan, N.K. Mondal, S. Chattoraj, Optimization using central composite design (CCD) and the desirability function for sorption of methylene blue from aqueous solution onto *Lemna major*, Karbala Int. J. Mod. Sci., 2 (2016) 145–155.
[21] A.R. Khatee, M. Fathinia, S. Aber, M. Zarei, Optimization of photocatalytic treatment of dye solution on supported TiO_2 nanoparticles by central composite design: intermediates identification, J. Hazard. Mater., 181 (2010) 886–897.
[22] A.S. Yusuff, Optimization of adsorption of Cr(VI) from aqueous solution by *Leucaena leucocephala* seed shell activated carbon using design of experiment, Appl. Water Sci., 8 (2018) 1–11.
[23] D. Jia, C. Li, Adsorption of Pb(II) from aqueous solutions using corn straw, Desal. Water Treat., 56 (2015) 223–231.
[24] S.F.S. Draman, N. Mohd, N.H.J. Wahab, N.S. Zulkfli, N.F.A.A. Bakar, Adsorption of lead(II) ions in aqueous solution using selected agro-waste, ARPN J. Eng. Appl. Sci., 10 (2015) 297–300.
[25] M.A. Njoki, G. Mercy, G. Nyagah, A. Gachanja, Fourier transform infrared spectrophotometric analysis of functional groups found in *Ricinus communis* L. and *Cucurbita maxima* Lam. roots, stems and leaves as heavy metal adsorbents, Int. J. Sci. Environ. Technol., 5 (2016) 861–871.
[26] M.N. Younis, M.S. Saeed, S. Khan, M.U. Surqan, R.U. Khan, M. Saleem, Production and characterization of biodiesel from waste and vegetable oil, J. Qual. Technol., 5 (2009) 111–121.
[27] C. Suresh, Y. Harinath, B.R. Naik, K. Seshaiah, Removal of Pb(II) from aqueous solution by critic acid modified *Manilkara zapota* leaves powder: equilibrium and kinetic studies, J. Chem. Pharm., 7 (2015) 1161–1174.
[28] P.A. Pednekar, B. Raman, The FT-IR spectrometric studies of vibrational bands of *Semecarpus anacardium* Linn. F. leaf, stem powder and extracts, Asian J. Pharm. Clin. Res., 6 (2013) 159–168.
[29] Z. Al-Qodah, R. Shawabkah, Production and characterization of granular activated carbon from activated sludge, Braz. J., 26 (2009) 127–136.
[30] G. Agrawal, P. Wakte, S. Shelke, Formulation optimization of human insulin loaded microspheres for controlled oral delivery using response surface methodology, Endocr. Metab. Immune Disord. Drug Targets, 17 (2017) 149–165.
[31] C. Garcia-Gomez, J.A. Vidales-Contreras, J. Npoles-Armenta, P. Gortares-Moroyoqui, Optimization of phenol removal using Ti/PbO_2 anode with response surface methodology, J. Environ. Eng., 142 (2016) 04016004 (1–7), doi: 10.1061/(ASCE) EE.1943-7870.0001057.
[32] A.O. Dada, A.P. Olalekan, A.M. Olatunya, O. Dada, Langmuir, Freundlich, Tempkin and Dubinin-Radushkevich isotherms studies of equilibrium sorption of Zn^{+2} unto phosphoric acid modified rice husk, IOSR J. Appl. Chem., 3 (2012) 38–45.